PROCEEDINGS OF THE 2015 ICONSSE ----

ISBN: 978-602-1047-217

PREPARATION AND CHARACTERIZATION OF NANOSIZE SPINEL NI0.9FE2CU0.1O4 USING PECTIN AS BINDING AGENT

Rodhiansyah Djayasinga, Rudy Situmeang

ABSTRACT

$Ni_{0.9}Fe_2Cu_{0.1}O_4$ nanomaterial have been prepared using a sol-gel method. Preparation of material was carried out by dissolving nitrate salts of iron, cobalt and nickel, in pectin solution and then the sample was stirred throughly using magnetic stirrer while adjusting pH to 11. After freeze-drying process, the sample was subjected to calcination treatment and subsequently characterized using the techniques of X-ray diffraction (XRD), Debye Scherrer Methods, PSA, and DT-TG analysis. The results of XRD characterizationand Rietveld calculation indicated that materials consist of four crystalline phases, such as, $CuFe_2O_4$, $Cu_{0,86}Fe_{2,14}O_4$, $NiFe_2O_4$, and NiO. The first three crystalline phases is superimposed. DT-TGA result showed that spinel $Ni_{0.9}Fe_2Cu_{0.1}O_4$ formed at 400^{o}C. Then, PSA determination proved that the grain size of spinel ferrites is a range of 30–95.2 nm as much as 21%. Crystallite size calculation using Scherrer equation, proved that the size is 35.42 nm and its size increased as temperature calcination inclined.

Keywords : Nanomaterial, BrØnsted–Lowry and Lewis acid sites, spinel ferrites

FULL TEXT:

PDF

REFERENCES

Boucheffa, Y., Benaliouche, F., Ayrault, P., Mignard, S., & Magnoux, P. (2008). NH3-TPD and FTIR Spectroscopy of pyridine adsorption studies for characterization of Ag- and Cu- exchanged X-zeolites. Microporous and Macroporous Material, 113(1–3), 80–88.

Candeiaa, R.A., Bernardi, M.I.B., Longoc, E., Santos, I.M.G., & Souzaa, A.G. (2004). Synthesis and characterization of spinel pigment CaFe2O4 obtained by the polymeric precursor method. Mater. Lett., 58, 569–572.

Cullity, B.D. (1978). Elements of X-ray diffraction (2nd Ed.). Addison–Wesley, London.

Corrias, A., Carta, D., Loche, D., Mountjoy, G., & Navarra, G. (2008). NiFe2O4 nanoparticles dispersed in an aerogel silica matrix: An X-ray absorption study. J. Phys. Chem. C, 112, 15623–15630.

Daadmehr, V., Akbarnejad, R. H., Rezakhani, A. T., Tehrani, F. S., Aghakhani, F., & Gholipour, S. (2013). Catalytic activity of the spinel ferrite nanocrystals on the growth of carbon nanotubes. J. Supercond. Nov. Magn., 26(2), 429–435.

Hill, R.J., Craig, J.R., & Gibbs, G.V. (1979). Systematics of the spinel structure type. Phys. Chem. Minerals, 4(4), 317–339.

Imanaka, N., Wendusu, Yoshida, T., & Masui, T. (2015). Novel environmentally friendly inorganic red pigments based on calcium bismuth oxides. J. Adv. Ceram., 4(1), 39–45.

Kumar, G.R., Kumar, K.V., & Venudhar, Y.C. (2012). Synthesis, structural and magnetic properties of copper substituted nickel ferrites by Sol–Gel method. Mater. Scie. Appl., 3(2), 87–91.

Le, M.-V., Dao, H.-A., Ken-Hirota, Masaki-Kato, Phuo, Huynh-Ky, H. (2014). Preparation and characterization of spinel co-doped MnAl2O4 obtained by Sol–Gel method. Proceedings of the 3rd World Conference on Applied Sciences, Engineering & Technology, Nepal, 709–715.

Maensiri, S., Masingboon, C., Bonochom, B., & Seraphin S. (2007). A simple route to synthesize nickel ferrite (NiFe2O4) nanoparticles using egg white. Script. Mat., 56, 797–800.

Murthy, Y.L.N., Viswanath, I.V.K., Rao, T.K., & Singh, R. (2009). Synthesis and characterization of nickel copper ferrite. Int.J. ChemTech Res., 1(4), 1308–1311.

Niyaifar, M., Nazari, S., & Mohammadpour, H. (2014). Magnetic and structural studies of Mg1-xZnxFe2O4. Proceedings of AES-ATEMA 18th Int. Conf., Canada, 203–212.

Parry, E.P. (1963). An Infrared study of pyridine adsorbed on acidic solids characterization of surface acidity. J. Catal., 2(5), 371–379.

Perego, C., & Villa, P. (1997). Catalyst preparation methods. Catal. Today, 34, 281–305.

Qian, F.Z., Jiang, J.S., Jiang, D.M., Wang, C.M., & Zhang, W.G. (2010). Improved multiferroic properties and a novel magnetic behavior of Bi0.8La0.2Fe1-xCoxO3 nanoparticles, J. Magn. Magn. Mater, 322(20), 3127–3130.

Malvern Instruments (2012). A basic guide to particle characterization. Malvern Instrument Limited, UK. Retreived from http://www.atascientific.com.au/publications/wp-content/uploads/2012/

/MRK1806-01-basic-guide-to-particle-characterisation.pdf.

Roy, A., Gupta, R., & Garg, A. (2012). Multiferroic memories. Adv. Condens. Matter Phys., 2012, 1–12.

Ryczkowski, J. (2001). IR spectroscopy in catalysis. Catalysis Today, 68, 263–381.

Situmeang, R., Wibowo, S., Simanjuntak, W., Supryanto, R., Amalia, R., Septanto, M., Manurung, P., & Sembiring, S. (2015a). Characteristics of nanosize spinel NixFe3-xO4 prepared by Sol–Gel method using egg white as emulsifying agent. J. Indones. Chem., 15(2), 116–122.

Situmeang, R., Manurung, P., Sulistiyo, S. T., Hadi, S., Simanjuntak, W., & Sembiring, S. (2015b). Sol–Gel method for preparation of nanosize NiFe2-xCoxO4 using egg white. Asian J. Chem., 27(3), 1138–1142.

Sutka, A., Borisova, A., Kleperis, J., Mezinskis, G., Jakovlevs, D., & Juhnevica, I. (2012). Effect of nickel addition on colour of nanometer spinel zinc ferrite pigments. J. Austral. Ceram. Soc., 48(2), 150–155.

Tanabe, K. (1970). Solid acids and bases: their catalytic properties. Kodansha, Tokyo.

Vanaja, M., Gnanajobitha, G., Paulkumar, K., Rajeshkumar, S., Malarkodi, C., & Annadurai, G. (2013). Phytosynthesis of silver nanoparticles by Cissus quadrangularis: influence of physicochemical factors. J. Nanostruct. Chem., 3(17), 1–8.

Waqas , H., Qureshi, A.H., Subhan, K., & Shahzad, M. (2012). Nanograin Mn–Zn ferrite smart cores to miniaturize electronic devices. Ceram. Internat., 38(2), 1235–1240.

Yehia, M., Labib, Sh., & Ismail, S.M. (2014). Structural and magnetic properties of nano-NiFe2O4 prepared using green nanotechnology. Physica B, 446, 49–54.

Yurdakoç, M., Akçay, M., Tonbul, Y., & Yurdakoç, K. (1999). Acidity of silica-alumina catalysts by amine titration using Hammett indicators and FT-IR study of pyridine adsorption. Turk. J. Chem., 23, 319–327.

REFBACKS

- There are currently no refbacks.

Proceedings of the 2015 IConSSE

ISBN: 978-602-1047-21-7

Preparation and characterization of nanosize spinel $Ni_{0.9}Fe_2Cu_{0.1}O_4$ using pectin as binding agent

Rodhiansyah Djayasinga[a] and Rudy Situmeang[b]

[a]*Graduate Student in Department of Chemistry, University of Lampung*
[b]*Department of Chemistry, University of Lampung*
Jln. Prof. Soemantri Brodjonegoro No. 1 Bandar Lampung 35145, Indonesia

Abstract

$Ni_{0.9}Fe_2Cu_{0.1}O_4$ nanomaterial have been prepared using a sol-gel method. Preparation of material was carried out by dissolving nitrate salts of iron, cobalt and nickel, in pectin solution and then the sample was stirred throughly using magnetic stirrer while adjusting pH to 11. After freeze-drying process, the sample was subjected to calcination treatment and subsequently characterized using the techniques of X-ray diffraction (XRD), Debye Scherrer Methods, PSA, and DT-TG analysis. The results of XRD characterizationand Rietveld calculation indicated that materials consist of four crystalline phases, such as, $CuFe_2O_4$, $Cu_{0,86}Fe_{2,14}O_4$, $NiFe_2O_4$, and NiO. The first three crystalline phases is superimposed. DT-TGA result showed that spinel $Ni_{0.9}Fe_2Cu_{0.1}O_4$ formed at 400°C. Then, PSA determination proved that the grain size of spinel ferrites is a range of 30–95.2 nm as much as 21%. Crystallite size calculation using Scherrer equation, proved that the size is 35.42 nm and its size increased as temperature calcination inclined.

Keywords : Nanomaterial, BrØnsted–Lowry and Lewis acid sites, spinel ferrites

1. Introduction

Spinel compounds have attracted great attention due to their many enormous properties for diverse industrial field applications, such as electronic devices [Waqas et al., 2012; Roy et al., 2012], magnetic materials [Niyaifar et al., 2014; Qian et al., 2010], pigments [Candeiaa et al., 2004; Imanaka et al., 2015], and catalysis [Daadmehr et al., 2013; Abelo et al., 2011, Situmeang et al., 2011]. In general, the applications of this spinel compound is governed by peculiar properties, which in turn depends on the chemical composition and microstructure [refs]. In general, the structural formula of spinel compound is symbolized as AB_2O_4 for II – III cation systems or A_2BO_4 for II-IV, II-III, I-III/IV cation systems (Le et al., 2014; Hill et al., 1979). Furthermore, the structural formula of spinel compound such as ferrites can be written as $(M^{2+}_{1-\delta}Fe^{3+}_{\delta})[M^{2+}_{\delta}Fe^{3+}_{2-\delta}]O_4$, where parentheses and square brackets denote cation sites of tetrahedral (A) and octahedral (B) coordination, respectively. δ, which is determined by the preparation process, represents the so called degree of inversion defined as the fraction of the (A) sites occupied by Fe^{3+} cations (Corrias et al., 2008; Lazarević et al., 2012; Sutka et al., 2012).

Since the choice of preparation method can determine the formation of a peculiar property of the material, it is crucial to decide which method of preparation will be used. Based on the literatures, sol-gel method is the better method compared to another method (Perego & Villa, 1997; Maensiri et al., 2007). This sol-gel method have proved that nano-materials will be formed (Yehia et al., 2014; Situmeang et al., 2015a,b). The nano-size

materials are really important and leads to the change of its properties that are needed to the various current and future specialized applications (Vanaja et al., 2013).

Spinel ferrites of $Ni_{1-x}Fe_2Cu_xO_4$ (x = 0.1–1) prepared by various method have been studied by several scientists (Kumar et al., 2012; Murthy et al., 2009; Daadmehr et al., 2013) and proved that the addition of Cu cation into spinel nickel ferrite will have a significant effect on the electromagnetic properties and catalytic functions. In this study we would like to report the preparation of nano spinel nickel copper ferrite, $Ni_{0.9}Fe_2Cu_{0.1}O_4$ prepared using sol-gel method and pectin as a binding agent. The materials obtained are characterized using XRD to identified the phases formed, PSA to know the particles sizes, Scherrer method to calculate crystallite sizes, and FTIR to identified both functional groups and bond formations.

2. Materials and Methods

2.1 Materials

Materials used in this work are pectin powder, $Ni(NO_3)_2.6H_2O$ (Merck, 99%), $Fe(NO_3)_3.9H_2O$ (Merck, 99%), $Cu(NO_3)_2.3H_2O$ (Merck, 99%), pyridine (C_5H_5N, J.T Baker), NH_3 (Merck, 99%), and aquadest.

2.2 Instrumentations

The instruments used for characterization were Fourier Transform Infrared (FTIR) spectrometer (Shimadzu Prestige-21) for identifying the presence of functional groups, and Differential Temperature and Gravimetry analysis (DT-GA) for elucidating the formation process . Then, a Philips X-ray diffractometer (XRD) model PW 1710 with Cu-Kα radiation was used for structural and crystalline phases identification and Particle Size Analyzer (PSA) for measuring particle size distribution.

2.3 Preparation of $Ni_{0.9}Fe_2Cu_{0.1}O_4$ nanomaterial

Stoichiometric amount of Ni (II) nitrate hydrates, Cu (II) nitrate hydrates and Fe (III) nitrate hydrates were dissolve in distilled water, having compositions $Ni_{0.9}Fe_2Cu_{0.1}O_4$ under magnetic stirring for 1 hour, respectively, followed by mixing each solution to make final solution weight ratio between nitrates to pectin is 3:2. Adjust the pH=11 in the above solution by addition of ammonia, and heat it at 80^{o}C with continue stirring to form viscous gel. Dried the gel using freeze dryer for 7 hours to form the precursors' networks and calcined at 600 and 800^{o}C for 3 hours. Finally Cu doped Ni - ferrite nanoparticles has prepared.

2.4 Characterization of $Ni_{0.9}Fe_2Cu_{0.1}O_4$ nanomaterial

Differential Temperature and Gravimetry Analysis

Sample of approximately 5–6 mg precursor was placed in Pt-sample compartment and the instrument was carried out under a flowing nitrogen atmosphere (50 ml/min, SII TG/DTA 7300). Then, scan analysis was worked in the range of 25 to 600^{o}C with ramp of 5^{o}C min^{-1}.

Particle Size Analysis

Particle size distribution of the solid sample is obtained by using the infra-red scattered through sample particles in ethanol media which was responding to the brownian movement on Beckman–Coulter Delsa nano. The principle of this analysis is accordance with *Dynamic Light Scattering* (DLS) method that is the smaller the particle the faster its moves.

The range of particle size could be measured is 0.1 nm to 10 μm. The result of particle size distribution is both calculated and analysed by using statistical method with *mean*, *median* and *modulus* parameters (Malvern Instruments, 2012).

X-*ray diffractogram analysis*

X-ray powder diffraction pattern of the sample was recorded from 2θ = 10 to 90° on a Philips diffractometer Model PW 1710 using Cu K_α radiation at a step 0.02° per second. The phase identification was performed using search and match method by comparing the x-ray pattern of the sample to those of the standards in the COD using Phase Identification from Powder Diffraction program Version-2. The particle size was also determined using Debye–Scherrer method (Cullity, 1978).

Acid sites analysis of $Ni_{0.9}Fe_2Cu_{0.1}O_4$

After heating at 120°C, sample was transferred into a crucible and placed in vaccumized dessicator. Pyridine was transferred into another crucible and placed in the dessicator to allow the vapour of the pyridine to contact with the sample. After 24 hours, the sample was taken from dessicator and left on open air for 2 hours to expell the physically adsorbed pyridine from the sample. Finally, the sample was analyzed using the FTIR spectroscopy. The analysis was conducted by grinding the sample with KBr of spectroscopy grade, and scanned over the wave number in the range of 4000–400 cm^{-1} (Parry, 1963; Ryczkowski, 2001).

3. Results and Discussion

3.1 Differential Temperature and Gravimetry Analysis

The precursor of $Ni_{0.9}Fe_2Cu_{0.1}O_4$ nanomaterial prepared were characterized using thermal analysis techniques such as differential temperature and thermal gravimetric analysis (DT-TGA). Thermal gravimetric analysis was used to measure the losses of weight as a function of temperature. The TGA results for the 4.8 h aged precursor containing [Cu]/[Ni]=1/9 molar ratio is shown in Figure 1.

There is a gradual weight loss upon heating to about 200°C; above this temperature there is a crucial weight loss until 400°C. During the first period of the weight loss, the exothermic process is occured at 173.7°C and the energy of 3.123 μVs/mg. The first weight loss with temperatures range of 100–200°C and is due to the removal of absorbed water in pectin networks. The second period of weight losses with temperatures at around 200–400°C, are considered to be due to the decomposition of pectin, and nitrate precursors, so that the decomposition at these high temperature regions produce water, carbon dioxides and nitrogen oxides simultaneously. Above 400°C, there was no weight loss and the formation of $Ni_{0.9}Fe_2Cu_{0.1}O_4$ nanomaterial was started.

3.2 X-ray diffractogram analysis

The prepared sample was characterized by Philips PW-1710 X-ray diffractometer using Cu-K_α radiation (λ =1.5406 Å) source. The X-ray diffraction pattern of the prepared sample is shown in Figure 2.

The diffraction pattern of $Ni_{0.9}Fe_2Cu_{0.1}O_4$ together with some standards related to the predicted phases of the sample was presented in Figure 2(a). With the aid of search and match method, using Phase Identification from Powder Diffraction program Version2, it was

found that the major phase is spinel $NiFe_2O_4$ (COD-96-230-0290), $CuFe_2O_4$ (COD-96-901-2439) and $Ni_{1.43}Fe_{1.7}O_4$ (COD-96-100-6117). Additional phase identified is spinel $NiFe_2O_4$ (COD-96-230-0296) as a minor phase. In general, it can be implied that both $NiFe_2O_4$ and $CuFe_2O_4$ crystalline phases are superimposed. By increasing the calcination temperature, the formation of both $CoFe_2O_4$ (JCPDF no. 34-0425) and $NiFe_2O_4$ (JCPDF no. 10-0325) were more pronounced by their intensities as indicated on Figure 2(b) above.

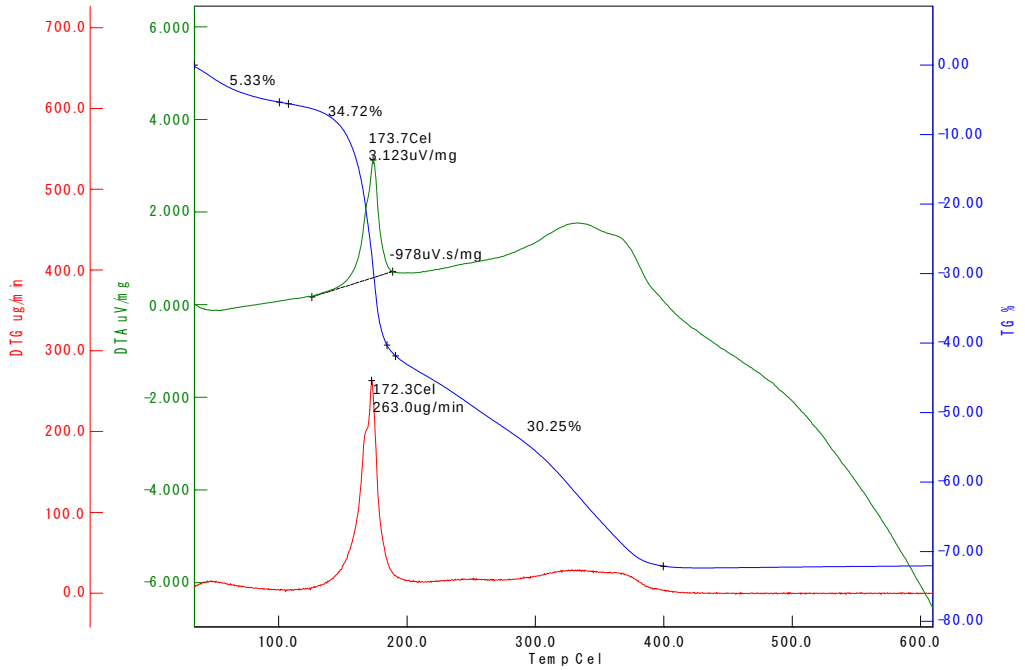

Figure 1. DT-TGA curve for $Ni_{0.9}Fe_2Cu_{0.1}O_4$ nanomaterial precursor with Cu/Ni = 1/9 molar ratio.

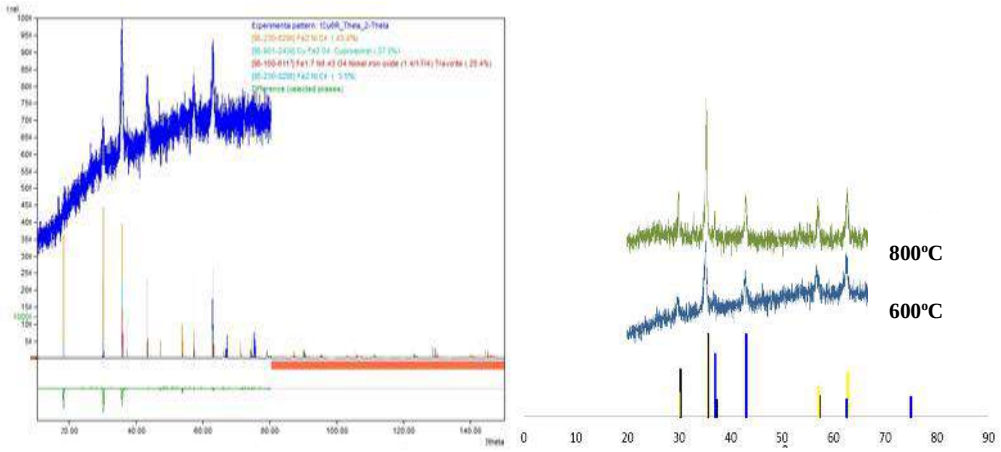

(a) (b)

Figure 2. (a) Difractogram of $Ni_{0.9}Fe_2Cu_{0.1}O_4$ nanomaterial after calcining at 600°C and (b) $Ni_{0.9}Fe_2Cu_{0.1}O_4$ nanomaterial after calcining 600 and 800°C.

Moreover, the crystallite size of $Ni_{0.9}Fe_2Cu_{0.1}O_4$ nanomaterial was calculated from the most prominent peak (211) of XRD using the Scherrer formula (Cullity, 1978):

$$D = \frac{k^{a}}{\beta \cos \theta_{\beta}},$$

where *D* is the crystallite size (nm), λ =1.5406 Å or 0.15406 nm is the wavelength of incident X-ray, θ_β is the diffraction angle at the prominent peak and β is the broadening of diffraction line measured at half maximum intensity, $\frac{®}{1}\ x\ F$ (in radian), and k is a constant with range of 0.9–1.0 (in this calculation, k = 0.94). θ is the Bragg's angle in degree unit. The calculation results are compiled in Table 1.

Table 1. Crystallite size calculation using Scherrer equation.

$Ni_{0.9}Fe_2Cu_{0.1}O_4$ Calcined at	2^{-} (deg)	hkl	FWHM		Size of Crystallite (D) (nm)
			degree	( )/ radian	
600°C	35.18	211	0.6984	0.012183	12.48
800°C	35.36	211	0.4571	0.007974	19.08

As shown in Table 1, the crystallite sizes of $Ni_{0.9}Fe_2Cu_{0.1}O_4$ samples are in the range of 10–20 nm, demonstrating the efficacy of the proposed method to produce nano-size spinel $Ni_{0.9}Fe_2Cu_{0.1}O_4$. In relation with the calcination variation, it was found that the higher the calcination temperature the bigger the crystallite size.

3.3 Particle Size Analysis

Figure 3 shows the particle size distribution of the $Ni_{0.9}Fe_2Cu_{0.1}O_4$ sample obtained at one angle of incidence of the laser beam (65°) by the particle size analyzer (PSA). It implies that the sample has a variety of particle sizes in both nano and micro scales with maximum intensity at certain sizes shown in Table 2. The average particle sizes of the sample estimated from PSA is also displayed in Table 2.

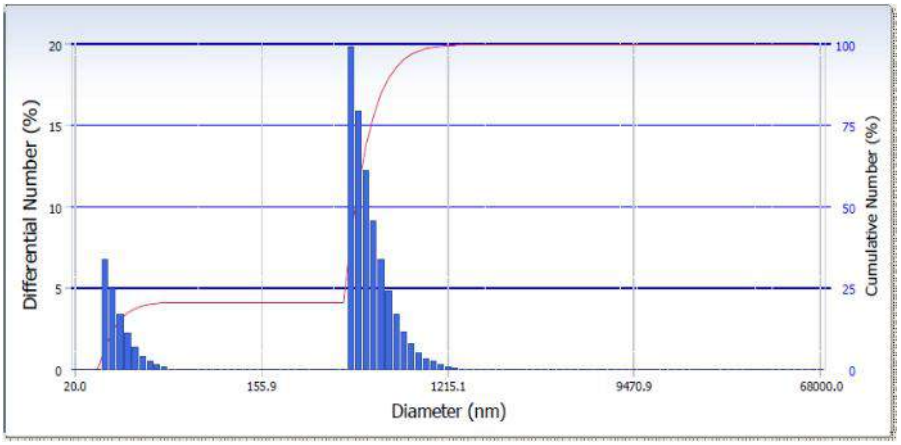

Figure 3. Particle size distribution of $Ni_{0.9}Fe_2Cu_{0.1}O_4$ nanomaterial sample.

The existence of micro scale can be concluded that the majority of particles tend to agglomerate, may be due to the lack of both pre-treatment on preparation of PSA sample and variation of incident angle of the laser beam. The values of the crystallite sizes calculated from the XRD patterns is actually all observed in the particle size distribution detected by the PSA. In other words, the particle size distribution detected by the PSA represents a grain size and enhances the calculated crystallite sizes from the XRD patterns.

Table 2. Particle size distribution and the average particle sizes of $Ni_{0.9}Fe_2Cu_{0.1}O_4$ sample estimated by PSA.

$Ni_{0.9}Fe_2Cu_{0.1}O_4$ calcined at 600 °C	Particle Size (nm)	Percentage of Particle sizes (%)	Average particle size Calculated from PSA data (nm)
Group 1	27.8	20.8	32.4
Group 2	417.7	79.2	530.7

3.4 Acid sites analysis of $Ni_{0.9}Fe_2Cu_{0.1}O_4$

Fourier transform infrared spectroscopy was applied to identify the functional groups present in the sample, primarily to identify the existence of Lewis and BrØnsted–Lowry acid sites. The acid sites identification is of particular importance since the acidity is acknowledged as very important characteristic which determine the performance of a material as a catalyst (Parry, 1963; Tanabe, 1970; Ryczkowski, 2001). The FTIR spectra of $Ni_{0.9}Fe_2Cu_{0.1}O_4$ sample investigated is shown in Figure 4.

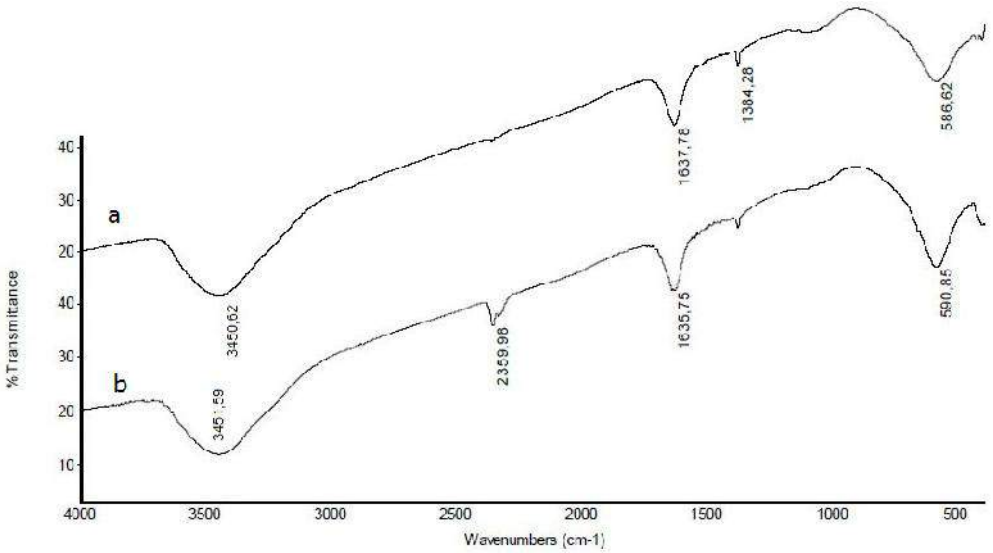

Figure 4. FTIR Spectrum of $Ni_{0.9}Fe_2Cu_{0.1}O_4$ after exposed to pyridine vapour: a. calcined at 600°C and b. calcined at 800°C.

As shown in Figure 4, In general, the peaks appeared at the wavelength range of 3500–3000 cm^{-1} are assigned to O-H stretching vibration, and the absorption bands located at 630–580 cm^{-1} and at 480–420 cm^{-1} are assigned to strong and weak strecthing vibrations of M-O modes, respectively (Parry, 1963; Ryczkowski, 2001; Yurdakoç et al., 1999). The presence of M-O modes is supported by the vibration band located at the wavelength of 570–560 cm^{-1}. The existence of BrØnsted – Lowry and Lewis sites is displayed by the absorption bands located at 1475–1420 cm^{-1} and 1620–1510 cm^{-1}, respectively (Yurdakoç et al., 1999; Boucheffa et al., 2008).

In the samples investigated, the presence of O-H functional group is indicated by the absorption band, resulted from stretching vibration, located at 3450.62 cm^{-1} . The existence of Lewis acid sites in the sample is displayed by the adsorption bands located at 1637.78 cm^{-1} which indicate that the pyridine was bound to the surface of the sample by coordination bond (Parry, 1963), while the existence of BrØnsted–Lowry acid sites is presented by the

absorption bands located at 1384.28 cm^{-1}. By comparing the intensities of the absorption bands associated with Lewis and BrØnsted–Lowry acid sites, it can be concluded that the acid characteristic of the sample is dominated by Lewis acid. In the fingerprint region of the spectra, the absorption band representing strecthing vibration of Fe-O and bending vibration of Ni-O and Cu-O was detected at 586.62, 450 and 430 cm^{-1} (Ryczkowski, 2001 ; Situmeang et al., 2015[b]), suggesting the existences of Fe-O-Ni and Fe-O-Cu bond which confirms the formation of $Ni_{0.9}Fe_2Cu_{0.1}O_4$ structure as expected.

4. Conclusion and remarks

This current study demonstrated the potential of pectin solution as a binding agent for preparation of nano-size materials using sol–gel method. The XRD results revealed that the crystallite size of the $Ni_{0.9}Fe_2Cu_{0.1}O_4$ sample prepared is in the range of 12 to 20 nm. The samples were found to exhibit Lewis and BrØnsted–Lowry acid characteristics, with Lewis acid as the dominant site, as revealed by the FTIR analyses. The agglomeration of $Ni_{0.9}Fe_2Cu_{0.1}O_4$ particles reflected by a microsize distribution in PSA is characterized by the existence of particles with varied sizes and shapes.

Acknowledgment

The authors wish to thank and appreciate the Health Ministry, Republic of Indonesia for research funding provided through Center for Standard and Certification, Health Polytechnics Program, Bandar Lampung.

References

Boucheffa, Y., Benaliouche, F., Ayrault, P., Mignard, S., & Magnoux, P. (2008). NH_3-TPD and FTIR Spectroscopy of pyridine adsorption studies for characterization of Ag- and Cu- exchanged X-zeolites. *Microporous and Macroporous Material*, *113*(1–3), 80–88.

Candeiaa, R.A., Bernardi, M.I.B., Longoc, E., Santos, I.M.G., & Souzaa, A.G. (2004). Synthesis and characterization of spinel pigment $CaFe_2O_4$ obtained by the polymeric precursor method. *Mater. Lett.*, *58*, 569–572.

Cullity, B.D. (1978). Elements of X-ray diffraction (2nd Ed.). Addison–Wesley, London.

Corrias, A., Carta, D., Loche, D., Mountjoy, G., & Navarra, G. (2008). $NiFe_2O_4$ nanoparticles dispersed in an aerogel silica matrix: An X-ray absorption study. *J. Phys. Chem. C*, *112*, 15623–15630.

Daadmehr, V., Akbarnejad, R. H., Rezakhani, A. T., Tehrani, F. S., Aghakhani, F., & Gholipour, S. (2013). Catalytic activity of the spinel ferrite nanocrystals on the growth of carbon nanotubes. *J. Supercond. Nov. Magn.*, *26*(2), 429–435.

Hill, R.J., Craig, J.R., & Gibbs, G.V. (1979). Systematics of the spinel structure type. *Phys. Chem. Minerals*, *4*(4), 317–339.

Imanaka, N., Wendusu, Yoshida, T., & Masui, T. (2015). Novel environmentally friendly inorganic red pigments based on calcium bismuth oxides. *J. Adv. Ceram.*, *4*(1), 39–45.

Kumar, G.R., Kumar, K.V., & Venudhar, Y.C. (2012). Synthesis, structural and magnetic properties of copper substituted nickel ferrites by Sol–Gel method. *Mater. Scie. Appl.*, *3*(2), 87–91.

Le, M.-V., Dao, H.-A., Ken-Hirota, Masaki-Kato, Phuo, Huynh-Ky, H. (2014). Preparation and characterization of spinel co-doped $MnAl_2O_4$ obtained by Sol–Gel method. *Proceedings of the 3rd World Conference on Applied Sciences, Engineering & Technology, Nepal*, 709–715.

Maensiri, S., Masingboon, C., Bonochom, B., & Seraphin S. (2007). A simple route to synthesize nickel ferrite ($NiFe_2O_4$) nanoparticles using egg white. *Script. Mat.*, *56*, 797–800.

Murthy, Y.L.N., Viswanath, I.V.K., Rao, T.K., & Singh, R. (2009). Synthesis and characterization of nickel copper ferrite. *Int.J. ChemTech Res.*, *1*(4), 1308–1311.

Niyaifar, M., Nazari, S., & Mohammadpour, H. (2014). Magnetic and structural studies of $Mg_{1-x}Zn_xFe_2O_4$. *Proceedings of AES-ATEMA 18th Int. Conf.*, *Canada*, 203–212.

Parry, E.P. (1963). An Infrared study of pyridine adsorbed on acidic solids characterization of surface acidity. *J. Catal.*, *2*(5), 371–379.

Perego, C., & Villa, P. (1997). Catalyst preparation methods. *Catal. Today*, *34*, 281–305.

Qian, F.Z., Jiang, J.S., Jiang, D.M., Wang, C.M., & Zhang, W.G. (2010). Improved multiferroic properties and a novel magnetic behavior of $Bi_{0.8}La_{0.2}Fe_{1-x}Co_xO_3$ nanoparticles, *J. Magn. Magn. Mater*, *322*(20), 3127–3130.

Malvern Instruments (2012). A basic guide to particle characterization. Malvern Instrument Limited, UK. Retreived from http://www.atascientific.com.au/publications/wp-content/uploads/2012/07/MRK1806-01-basic-guide-to-particle-characterisation.pdf.

Roy, A., Gupta, R., & Garg, A. (2012). Multiferroic memories. *Adv. Condens. Matter Phys.*, *2012*, 1–12.

Ryczkowski, J. (2001). IR spectroscopy in catalysis. *Catalysis Today*, *68*, 263–381.

Situmeang, R., Wibowo, S., Simanjuntak, W., Supryanto, R., Amalia, R., Septanto, M., Manurung, P., & Sembiring, S. (2015a). Characteristics of nanosize spinel $Ni_xFe_{3-x}O_4$ prepared by Sol–Gel method using egg white as emulsifying agent. *J. Indones. Chem.*, *15*(2), 116–122.

Situmeang, R., Manurung, P., Sulistiyo, S. T., Hadi, S., Simanjuntak, W., & Sembiring, S. (2015b). Sol–Gel method for preparation of nanosize $NiFe_{2-x}Co_xO_4$ using egg white. *Asian J. Chem.*, *27*(3), 1138–1142.

Sutka, A., Borisova, A., Kleperis, J., Mezinskis, G., Jakovlevs, D., & Juhnevica, I. (2012). Effect of nickel addition on colour of nanometer spinel zinc ferrite pigments. *J. Austral. Ceram. Soc.*, *48*(2), 150–155.

Tanabe, K. (1970). *Solid acids and bases: their catalytic properties*. Kodansha, Tokyo.

Vanaja, M., Gnanajobitha, G., Paulkumar, K., Rajeshkumar, S., Malarkodi, C., & Annadurai, G. (2013). Phytosynthesis of silver nanoparticles by Cissus quadrangularis: influence of physicochemical factors. *J. Nanostruct. Chem.*, *3*(17), 1–8.

Waqas , H., Qureshi, A.H., Subhan, K., & Shahzad, M. (2012). Nanograin Mn–Zn ferrite smart cores to miniaturize electronic devices. *Ceram. Internat.*, *38*(2), 1235–1240.

Yehia, M., Labib, Sh., & Ismail, S.M. (2014). Structural and magnetic properties of nano-$NiFe_2O_4$ prepared using green nanotechnology. *Physica B*, *446*, 49–54.

Yurdakoç, M., Akçay, M., Tonbul, Y., & Yurdakoç, K. (1999). Acidity of silica-alumina catalysts by amine titration using Hammett indicators and FT-IR study of pyridine adsorption. *Turk. J. Chem.*, *23*, 319–327.